A High Efficiency 750 V/ 100 A Cryogenically Cooled Solid State Circuit Breaker Module for Aviation Applications

Ching-Hsiang Yang
CURENT
University of Tennessee
Knoxville, USA
cyang30@vols.utk.edu

Shimul K. Dam
CURENT
University of Tennessee
Knoxville, USA
sdam@utk.edu

Zhou Dong
ABB US Research Center
ABB. Inc
Raleigh, USA
zhou.dong@us.abb.com

Dehao Qin
Clemson University
North Charleston, USA
dehaoq@g.clemson.edu

Ruirui Chen
CURENT
University of Tennessee
Knoxville, USA
rchen14@vols.utk.edu

Fred Wang
CURENT
University of Tennessee
Oak Ridge National Laboratory
Knoxville, USA
fred.wang@utk.edu

Hua Bai
CURENT
University of Tennessee
Knoxville, USA
hbai2@utk.edu

Zheyu Zhang
Rensselaer Polytechnic Institute
Troy, NY, USA
zhangz49@rpi.edu

Abstract— **A solid-state circuit breaker (SSCB) needs to have very high efficiency comparable to its mechanical counterpart, and GaN offers highest conduction loss reduction at cryogenic temperatures. So, cryogenic cooling of future EAP is leveraged to design a 750V/100A SSCB module with an efficiency target higher than 99.9% and high over-current capability. The cryogenically cooled SSCB module design is developed in this paper, including key components selection and module design considerations. Experimental results are provided to validate the capability of the designed SSCB module to interrupt 10x of rated current at cryogenic temperatures (<-153^{0}C).**

Keywords— GaN HEMTs, paralleled GaN HEMTs, solid-state circuit breaker, cryogenic.

I. INTRODUCTION

Future Electrified Aircraft Propulsion (EAP) system requires power electronic systems with high efficiency, high power density, low weight, and high reliability. The emerging wide-bandgap (WBG) semiconductors, such as silicon carbide (SiC) and gallium nitride (GaN), can improve power electronic performances compared to the Si counterparts, e.g., lower loss, faster switching, smaller size, and wider temperature capability. Besides, the cryogenic coolant in the future EAP system can be utilized to further reduce the loss and increase the power density of the power electronics systems. Future EAP systems are expected to use an MVDC power distribution system due to high power requirements. Fast fault protection is essential for such a system due to higher voltage and lower line inductance. SSCB must be utilized to achieve sufficient fault clearance speed. Compared to the mechanical and hybrid breakers, SSCB has advantages of fast current interruption, size and weight reduction, and providing additional functions [1][2], but offers lower efficiency. This work aims at improving efficiency and over-current capability of SSCB significantly by utilizing cryogenic cooling and superior performance of WBG devices.

GaN High Electron Mobility Transistor (HEMT) is reported to offer more conduction loss reduction at cryogenic temperature (<-153°C) compared to Si and SiC devices [3]. Several GaN based SSCBs have been reported [4]-[7]. However, none of these leverage the large conduction loss reduction of GaN device under cryogenic cooling and the power ratings are relatively low in comparison to future EAP system requirements, which is expected to be medium voltage and MW power levels [8].

This article proposes a cryogenically cooled GaN-HEMT based SSCB module which can achieve higher than 99.9% efficiency and high over-current interruption capability using only two GaN dies in parallel. The designed SSCB module is rated at 750 V/ 100 A and can be connected in series and/or parallel for higher power ratings. The maximum current interruption for each module is 1 kA, which is 10x of the rated current. Moreover, the SSCB module is designed to be cooled at cryogenic temperature using liquid nitrogen (LN2), i.e., -180°C during rated current operation.

This paper is organized as follows. Section II presents the selection criteria of main components including power semiconductor devices and voltage clamping circuits. In section III, the design of the proposed SSCB module would be addressed. Section IV demonstrates the test result of the designed SSCB module. Section V concludes the paper.

II. Main Components Selection

A typical SSCB topology is shown in Fig. 1, which consists of the power devices, voltage clamping circuit or energy absorb unit (EAU), gate driver, auxiliary power supply and sensing circuits. In a typical SSCB switching operation, semiconductor devices stay in ON-state during normal conditions. When any overload or fault is detected, devices are turned off and the voltage is built up by the residual energy remaining in the system inductances. Once the voltage reaches a certain value, the voltage clamping circuit is activated to keep the voltage at a safe level for semiconductor devices, and also to take up the remaining energy until the system current reduce to zero.

The power devices and the EAUs are two of the main components that handle the power in SSCB. Thus, the selection of these main components is critical to achieve high efficiency and required voltage and current ratings of the application.
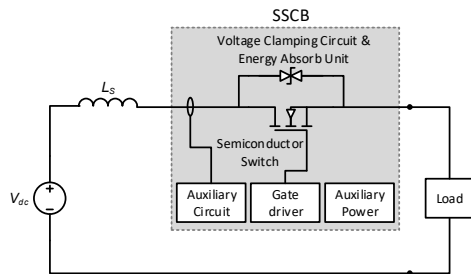

Fig. 1. Typical SSCB in a DC system

A. Power Devices

WBG devices such as SiC MOSFETs and GaN HEMTs are known for their low specific on-resistance compared to Si counterparts, which is beneficial to the SSCB applications. However, SiC MOSFETs are reported to have an increased on-resistance with decreased temperatures, different from Si MOSFETs and GaN HEMTs [9]. The increased on-resistance generates a higher conduction loss. On the other hand, GaN HEMTs, compared to Si MOSFETs, exhibit lower specific on-resistance both at room temperature and low temperature range. Moreover, GaN HEMTs do not exhibit the carrier freeze out effect, which prevents the on-resistance of Si MOSFETs from further reducing at lower temperatures. Besides, GaN HEMTs also show a constant breakdown voltage from room temperature to cryogenic temperatures, while Si MOSFETs show reduced breakdown voltage. As a result, GaN HEMTs have the lowest specific on-resistance and stable breakdown voltage when temperatures drop, which are suitable for the cryogenically cooled circuit breaker applications.

The low on-resistance of GaN HEMTs at low temperature results in low conduction loss thereby high efficiency when the SSCBs operate at the normal condition. Moreover, the positive temperature coefficient of on-resistance is also beneficial for device parallelization to increase the overall current rating of the SSCB module. Fig. 2 shows the I-V characteristic and the on-resistance of the candidate 650 V, 150 A GaN HEMTs, GS-065-150 from GaN Systems at different temperature with 6 V gate voltage, measured by Keysight B1505A. Fig 2(a) shows

that these GaN HEMTs are saturated ~300 A at the room temperature. As the temperature decreases, the slopes of I-V curve increase and stay in the ohmic region, which indicates the reduction of the on-state resistance. Also, a steeper I-V curve shows the device can allow higher current at lower temperature without any saturation. The higher current capability at lower temperature enables GaN based cryogenically cooled SSCBs to withstand more transient current when the fault occurs. Fig. 2(b) presents the positive temperature coefficient of on-resistances of GaN HEMTs. The resistance is reported to be around 11.5 mΩ at room temperature and 2.3 mΩ at -180°C, which is about one-fifth of that at the room temperature.

For the SSCB module rated at 100 A with 10x current interrupting capability, only two paralleled GS-065-150 are required. Although paralleling more devices can have better efficiency and higher current capability, more cost and complexity would be added to the circuit design. With more than two devices in parallel, circuit must be carefully designed to prevent non-identical loop or extra loop inductance. Since GaN HEMTs are very sensitive to parasitics, these non-identical loop and extra parasitics introduced from the circuit can result in current unbalance among devices, or even create unwanted ringing during transitions that can potentially lead to the device failure. With two GaN-HEMTs in parallel, the overall on-resistance would be 1.15 mΩ with cryogenic cooling. The efficiency of the 100 A SSCB module could be greater than 99.9%.
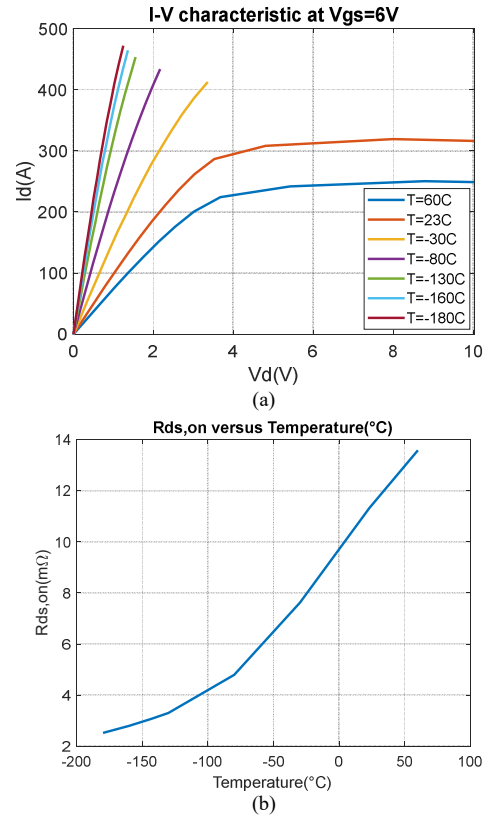

(a)

(b)

Fig. 2. Characteristics of GS-065-150 (a) I-V at different temperature (b) Rds(on) versus temperature.

B. Voltage Clamping Circuits

The SSCB requires voltage clamping circuits to withstand the voltage across the semiconductor switch whenever the breaker turns off. Furthermore, it should also be capable of absorbing the residual energy in the system inductance. The design of the voltage clamping circuit should consider clamping voltage, peak current, and energy absorbing capability. Typical options of the voltage clamping and energy absorption circuits can be categorized as linear components as snubbers circuits, and non-linear solutions such as metal oxide varistor (MOV) and transient voltage suppression (TVS) diode [10].

An RC snubber is the simplest voltage clamping solutions. However, the voltage drop across snubber resistors will also reflect on the voltage stress across the power devices. Adding a diode in parallel with the resistor can avoid the additional voltage drops but would also increase the complexity of design and might reduce the reliability [11], [12].

MOV and TVS diodes are two non-linear solutions for voltage clamping and energy absorption. MOVs utilize the characteristics of nonlinear resistance as a function of voltage. The resistance of the MOV is very high at low voltage and drops to very low value once the voltage enters the clamping region. When the breaker turns off, the voltage reaches the clamping region and the energy is dissipated in the MOV. Then the breaker voltage gradually decreases until it goes back to the system voltage. With the proper design, MOV can assure a safe clamping voltage for power semiconductor devices. However, MOVs have the degradation issue in the energy absorption process [13]-[15]. The limited lifetime and reliability issue of MOVs might be undesirable in aviation applications. The TVS diode, on the other hand is more attractive compared to the commonly used MOV due to the faster response speed, lower clamping ratio, and higher reliability without degradation.

The high power TVS diode has foldback characteristics shown in Fig. 3, where the voltage reaches a peak value initially and falls to an average clamping voltage. The high clamping ratio between the peak and the average voltage results in a longer interrupting time and higher voltage stress on switching devices. However, the clamping ratio of the high power TVS diode decreases at cryogenic temperatures, as shown in Fig. 4. At cryogenic temperature, the lower peak clamping voltage can reduce the voltage stress on semiconductor switches, and the higher average clamping voltage can accelerate system current to zero. In this design, two TVS diodes AK3-430C and AK3-150C from Little Fuse are connected in series. The designed peak clamping voltage is 640 V, which is slightly lower than the devices 650 V rating. The average clamping voltage is around 473 V for each GaN device at -180∘C.

C. RC Snubber

During the high current fault condition, the hard switching of the GaN HEMT can lead to large power dissipation that causes damage to the GaN dies. Fig. 5 shows the high current turn-off failure of the GaN HEMTs. Although an RC snubber can also be used as EAU in the SSCB application, it is designed here to limit the dv/dt during turn-off and the peak voltage across the power device. Also, by slowing down the voltage rising rate, the

transient power dissipation can be reduced in the device. This can prevent possible thermal failure when turning off a high fault current, e.g., 10x fault current. Fig. 6 shows the device turn-off waveforms with and without the snubber. It can be noted that the voltage rise without snubber is steeper with some oscillation, and the peak voltage can reach over 600 V. The power dissipation is also reduced significantly. Another benefit of adding the snubber is to mitigate the instability issue of paralleled devices [16]. Introducing the snubber capacitor can alleviate hard-switching stress at high current turn-off that is prone to have the instability. Since a single C snubber may oscillate with the stray inductance, an additional small resistor is added to damp the oscillations. In this design, a snubber with 0.5
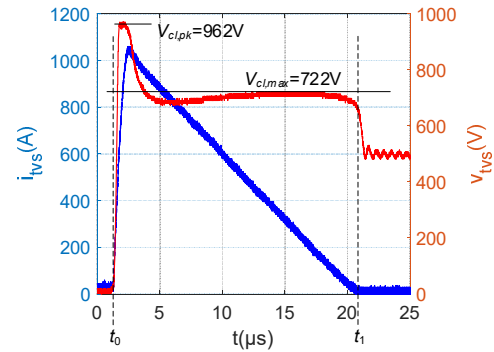

Fig. 3. Test waveforms of GaN HEMT turning off high currents
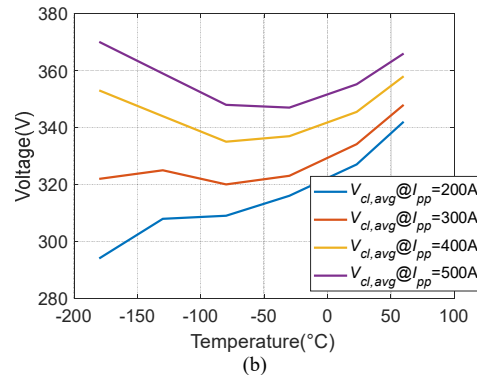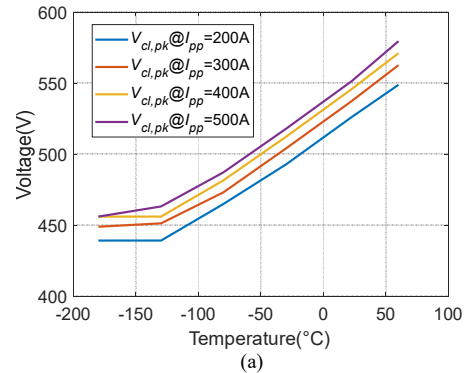

Fig. 4. Characteristics of high power TVS at different temperature (a) peak clamping voltage (b) average clamping voltage.
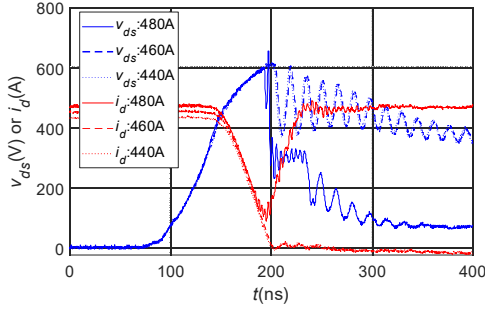
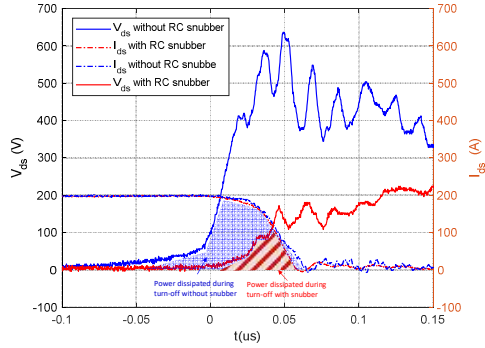Fig. 5. Test waveforms of the GaN HEMT turning off high currents

Fig. 6. Turn-off waveforms with/without an RC snubber

Ω resistor and 150 nF capacitor is selected considering the requirement of interrupting the high fault current up to 1 kA.

III. SSCB MODULE DESIGN

Fig. 7 shows the schematic diagram of the proposed SSCB module design. Two GaN HEMTs are in parallel to increase the current ratings. Two sets of such paralleled power devices are in series to increase the voltage ratings. The voltage clamping circuit, which consists of a TVS diode set and an RC snubber, is in parallel with each device to form a cell. The cell design can prevent uneven loop inductance between paralleled devices and TVS diodes, or RC snubber, when assembling the clamping circuit only at one side, as shown in Fig. 8. The uneven loop inductance would introduce unwanted ringing when current commutating from devices to the voltage clamping circuit, which may lead to device failures.

The layout of the GaN based circuit should be carefully designed to minimize the gate-loop and power-loop inductance. As shown in Fig. 9, the gate-drive circuit is placed in the middle of paralleled GaN HEMTs to ensure the identical gate loop. An RC snubber and TVS diode are placed close to each power device to reduce the power-loop inductance. The selected TVS diodes AK3-430C and AK3-150C are packaged with long lead, with its 3D view shown in Fig. 9. In order to minimize the effect of the lead pins, a "V-shape" alignment is designed in this module. One end of the two TVS diodes can be soldered directly on the drain and source pads, while the other two ends can be tied together. This eliminates the extra traces on the PCB to prevent additional stray inductance.
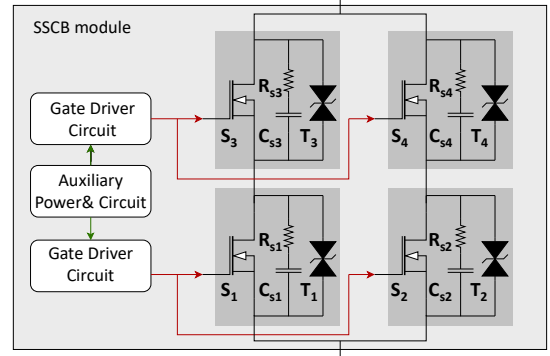

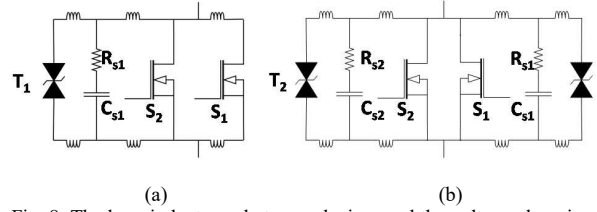
Fig. 7. Schematics of SSCB

(a)   (b)

Fig. 8. The loop inductance between devices and the voltage clamping unit (a) single voltage clamping circuit (b) voltage clamping circuit on each device.
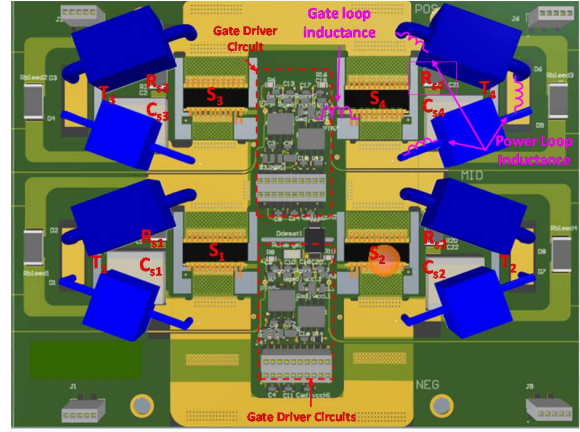

Fig. 9. Layout of the proposed SSCB

IV. EXPERIMENT RESULT

The proposed 750 V/ 100 A SSCB module is built and shown in Fig. 10(a). Each GaN HEMT die is in parallel with series connected TVS diodes (AK3-430C and AK3-150C) and RC snubber. The compact design of the SSCB aims to minimize the gate loop and the power loop, and to shrink the module size. The functionalities of the SSCB module are tested at both room and cryogenic temperature. The test setup is shown in Fig. 10(b). LN2 is utilized as a coolant to fill in the chamber. The SSCB module is placed in the chamber to emulate the temperature of the cryogenically cooled system.
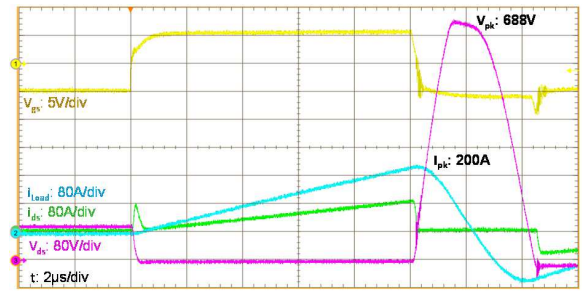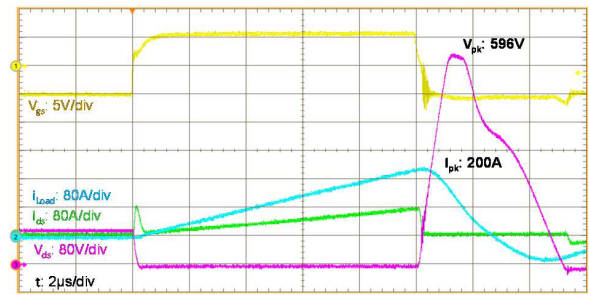
1748
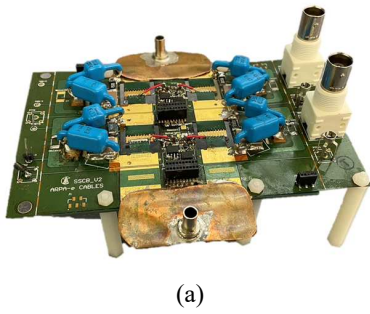
(a)
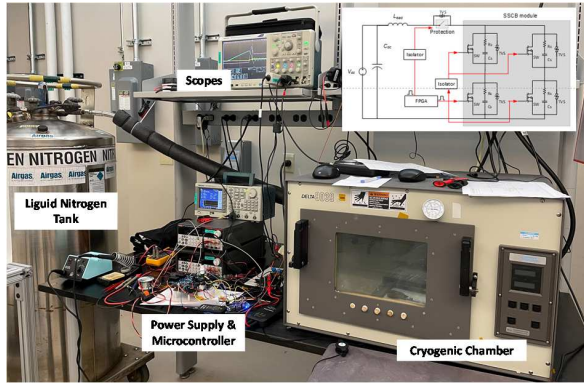
(b)

Fig. 10. (a) Designed SSCB module (b)Test setup of prototype SSCB module turn-off test
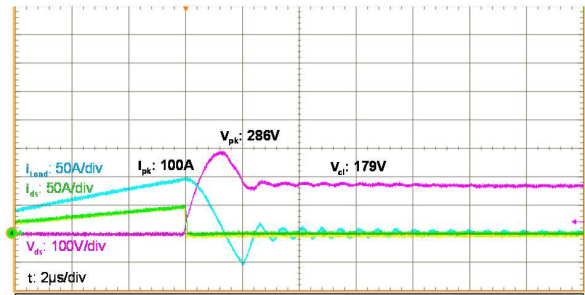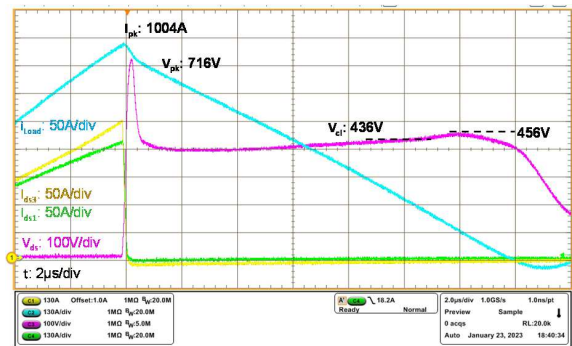

(a)

(b)

Fig. 11. Prototype SSCB turning-off 200 A current (a) at room temperature (b) at -180°C

(a)

(b)

Fig. 12. Prototype SSCB turning-off (a) 100 A current (b) 1 kA current at -180°C

Fig. 11 shows the test results of the proposed SSCB interrupting 200 A current at room temperature and at cryogenic temperature. The peak TVS voltage recorded is 688 V at room temperature, which is slightly higher than the device ratings. Since the selected device can withstand 750 V for 1μs, the device is not damaged because the voltage drops below 650 V in less than 1μs. However, the high peak voltage is reducing as temperature drops, where the peak TVS voltage is 596 V at -180°C. The results show the decreased peak clamping voltage of TVS diodes at lower temperature, which is good for reducing the voltage stress across the power devices.

Fig. 12 shows the prototyped SSCB module turning off rated 100 A and 10x rated current, which is 1 kA at -180°C. The peak clamping voltage is 716 V, higher than the designed 640 V. The reason for the higher clamping voltage is due to the packaged TVS diodes, where the existing lead introduces additional inductance between TVS diodes and main switches. During the commutations between the power device and the voltage clamping circuits, the high di/dt can lead to transient voltage spike. The inductance of the TVS lead is minimized by using the V-shape alignment in this design and can be further reduced by using the TVS bare dies. The average clamping voltage at -180°C is around 430 V, slightly lower than the designed value. This difference is because of the data point taken in the measurement. From Fig. 12(b), the voltage across the TVS diode is not at a constant level. Instead, the voltage increases after the foldback characteristic. At the end of the clamping period, the voltage is reported to be 456 V. Besides, the TVS

1749

diode voltage is a function of the junction temperature, which would also affect the reading.

The efficiency test of the prototyped SSCB module is conducted at -180°C in the chamber by applying constant gate voltage to all the power devices, and gradually increase the current flowing through the system by a DC power source in the constant current mode. A 300 W, 0.36 Ω load is connected in series with the prototype module. The loss is calculated by measuring the voltage drop across the SSCB module multiplied by the constant current from the source. The overall SSCB module resistance and efficiency are shown in Fig. 13. With four devices, two in parallel and two in series, the overall module resistance should be around 2 mΩ based on the characterization result in Section II. Fig. 13(a) shows that the module overall resistance meets the expectation, with 2 mΩ at low current, and increases to 3 mΩ due to the junction temperature rise. The efficiency of the module is measured to be over 99.9% up to 80 A, shown in Fig. 13(b). A better way to test the module is to use a cold plate with LN2 flows instead of a thermal chamber. The new test setup for the test is under development and the results will be reported in future.
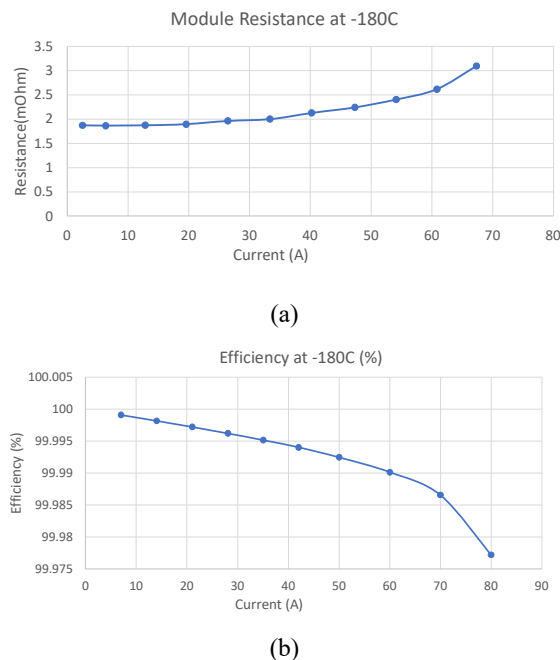

(a)

(b)

Fig. 13. Results of the module efficiency test (a) module overall resistance (b) module efficiency at -180°C

V. CONCLUSION

A GaN-based cryogenically cooled 750 V/ 100 A SSCB module is proposed. The key components are selected based on components characteristics at cryogenic temperature and specification requirements. The proposed SSCB module is developed and tested at both room temperature and cryogenic temperature. Experimental results validated the capability of the proposed SSCB to interrupt up to 1kA fault current. The measured efficiency is >99.9% up to 80 A for the prototype SSCB module. The improved cooling method is under development and the better efficiency number can be expected in the future.

REFERENCES

[1] P. J. Ansell, "Hydrogen-Electric Aircraft Technologies and Integration: Enabling an environmentally sustainable aviation future," in IEEE Electrification Magazine, vol. 10, no. 2, pp. 6-16, June 2022, doi: 10.1109/MELE.2022.3165721.

[2] F. F. Wang, R. Chen and Z. Dong, "Power Electronics: A critical enabler of future hydrogen–electric systems for aviation," in IEEE Electrification Magazine, vol. 10, no. 2, pp. 57-68, June 2022, doi: 10.1109/MELE.2022.3165954.

[3] H. Gui et al., "Review of Power Electronics Components at Cryogenic Temperatures," in IEEE Transactions on Power Electronics, vol. 35, no. 5, pp. 5144-5156, May 2020, doi: 10.1109/TPEL.2019.2944781.

[4] Y. Zhou, R. Na, Y. Feng and Z. J. Shen, "GaN-based tri-mode intelligent solid-state circuit breakers for low-voltage DC power networks", IEEE Trans. Power Electron., vol. 36, no. 6, pp. 6596-6607, Jun. 2021.

[5] G. E. Mejia-Ruiz, M. R. A. Paternina, A. Zamora-Mendez, J. C. Rosas-Caro and G. Bolivar-Ortiz, "A Novel GaN-Based Solid-State Circuit Breaker With Voltage Overshoot Suppression," in IEEE Transactions on Industrial Electronics, vol. 69, no. 9, pp. 8949-8960, Sept. 2022, doi: 10.1109/TIE.2021.3116557.

[6] Q. Kong, S. Wu, F. Zhang, P. Yang, Y. Zhou and J. Wei, "DC solid state circuit breaker based on GaN", Proc. 15th IEEE Conf. Ind. Electron. Appl., pp. 675-680, 2020.

[7] A. Suzuki, T. Ichiryu, Y. Kinoshita, H. Ishida, H. Handa and T. Hatsuda, "300 A Solid State Circuit Breaker using Parallel Connected GaN Bidirectional Switch," PCIM Europe digital days 2020; International Exhibition and Conference for Power Electronics, Intelligent Motion, Renewable Energy and Energy Management, Germany, 2020, pp. 1-6.

[8] R. Jansen, C. Bowman, A. Jankovsky, R. Dyson and J. Felder, "Overview of NASA electrified aircraft propulsion (EAP) research for large subsonic transports," in 53rd AIAA/SAE/ASEE Joint Propuls. Conf., 2017.General Standard for SSPC, SAE Aerospace Standard AS4805, 2007.

[9] R. Chen and F. F. Wang, "SiC and GaN Devices With Cryogenic Cooling," in IEEE Open Journal of Power Electronics, vol. 2, pp. 315-326, 2021, doi: 10.1109/OJPEL.2021.3075061.

[10] R. Rodrigues, Y. Du, A. Antoniazzi and P. Cairoli, "A Review of Solid-State Circuit Breakers," in IEEE Transactions on Power Electronics, vol. 36, no. 1, pp. 364-377, Jan. 2021, doi: 10.1109/TPEL.2020.3003358.

[11] F. Liu, W. Liu, X. Zha, H. Yang and K. Feng, "Solid-State Circuit Breaker Snubber Design for Transient Overvoltage Suppression at Bus Fault Interruption in Low-Voltage DC Microgrid," in IEEE Transactions on Power Electronics, vol. 32, no. 4, pp. 3007-3021, April 2017, doi: 10.1109/TPEL.2016.2574751.

[12] J. Magnusson, R. Saers, L. Liljestrand and G. Engdahl, "Separation of the Energy Absorption and Overvoltage Protection in Solid-State Breakers by the Use of Parallel Varistors," in IEEE Transactions on Power Electronics, vol. 29, no. 6, pp. 2715-2722, June 2014, doi: 10.1109/TPEL.2013.2272857.

[13] Microsemi Application Note: "An introduction to transient voltage suppressor devices", [Online]. Available: https://www.microsemi.com/document-portal/doc_download/14604-micronote-102-an- introduction-to-tvs-devices

1750

[14] K. P. Mardira, et. al, "Investigation of diagnostic techniques for metal oxide surge arresters," IEEE Trans. Dielectr. Electr. Insul., vol 12, no. 1, pp. 50-59, 2005.

[15] M. Mashaba and K. Nixon, "Deducing metal oxide varistor life span from pulse rating curves for surges of different magnitudes," ICHVE, pp.1-4, 2016.

[16] Z. Dong, R. Ren, W. Zhang, F. F. Wang and L. M. Tolbert, "Instability Issue of Paralleled Dies in an SiC Power Module in Solid-State Circuit Breaker Applications," in IEEE Transactions on Power Electronics, vol. 36, no. 10, pp. 11763-11773, Oct. 2021, doi: 10.1109/TPEL.2021.3068608.